Eng. Sci., 2022, **20**, 296–305

Engineered Science

DOI: https://dx.doi.org/10.30919/es8d761

Temperature Effects on Thermal Transport at the Graphene-liquid Interface

Hao Chen,[1, 2,†] Ming Yang,[2, 3,†] Degao Qiao,[1] Xingli Zhang[1,*] and Hang Zhang[2, 3,*]

Abstract

The mechanism of thermal resistance between graphene layers and nanofluids is essentially important to the performance and reliability of the graphene microchannels. In this paper, the interfacial thermal resistance of the graphene-water, graphene-ethanol, and graphene-ethylene glycol systems are systematically investigated using non-equilibrium molecular dynamics simulations (NEMD). The results showed that the interfacial thermal resistance of the three structures showed different trends as the temperature increased. The interfacial thermal resistance of the graphene-water, the graphene-ethanol, and the graphene-glycol system achieve a minimum value at 285 K, 165 K, and 335 K, respectively. The effects of graphene width on graphene-water interfacial thermal resistance are greater than that of graphene-ethanol and graphene-ethylene glycol systems, however, the thickness of the liquid cluster has greater effect on the interfacial thermal resistance for the graphene-ethanol and graphene-ethylene glycol interfaces than that of graphene-water system. The near-wall density analysis and phonon density of states analysis are calculated to explain the validity of our NEMD simulation results. Our study is helpful for improving the efficiency of the graphene microchannels.

Keywords: Molecular dynamics simulation; Thermal resistance; Phonon transport; Nanoscale system.
Received: 07 June 2022; Revised: 19 June 2022; Accepted: 22 July 2022.
Article type: Research article

1. Introduction

The graphene microchannel with superior high-temperature stability,[1] outstanding mechanical properties,[2] and rapid heat transfer[3] has inspired massive interest in the thermal engineering fields of electronic devices and thermoelectric devices.[4-17] Understanding and predicting interfacial thermal resistance between graphene layers and nanofluids is essential to further the advance of these graphene-based nanoscale devices. At the nanoscale, the underlying physical mechanisms for the thermal transport at the solid-liquid interface are complicated. The mechanisms can be concluded as follows: systematically the van der Waals interaction at the interfaces,[18] the surface imperfection[19] and phonon scattering,[20] and the phonon attenuation due to the phonon scatterings.[21-23] The main factors that govern the interfacial heat transport across the solid-liquid interface are the bonding strength,[24] temperatures,[25-27] and surface size.[28-30]

Thermal transport across the solid-liquid interface has been studied intensively since the discovery of Kapitza resistance.[31-35] Molecular dynamics simulation (MD) as a classical approach has many unique advantages to simulate thermal transport.[36] Konatham[37] investigated the thermal transport properties between graphene and liquid octane through molecular dynamics simulations, revealing that edge functionalization does not impair the heat transfer properties of graphene. Jian *et al*.[38] measured the thermophysical properties of graphene-containing nanofluids and explored the effect of temperature on their thermal transport properties. This new ionic liquid nanofluid has excellent potential as a heat transfer fluid. Pham[39] investigated the Kapitza length at the interface between the surface of graphene-coated copper nanocomposites and liquid water. The dramatic change in thermal resistance with the addition of single graphene was confirmed, showing that a single layer of graphene only allows 18% of the van der Waals energy under copper to be transported. Babaei[40] used molecular dynamics simulations to investigate the interfacial thermal resistance between graphene and paraffin in different states using non-equilibrium state simulations for parallel and perpendicular

[1] *College of Mechanical and Electrical Engineering, Northeast Forestry University, Harbin 150040, China.*
[2] *Institute of Engineering Thermophysics, Chinese Academy of Sciences, Beijing 100190, China.*
[3] *University of Chinese Academy of Sciences, Beijing 100049, China.*
†These authors contributed equally to this work.
**E-mail:* zhang-xingli@nefu.edu.cn (X. Zhang), zhanghang@iet.cn (H. Zhang)

configurations of graphene-paraffin, respectively. Peng *et al*.[41] calculated the thermal resistance of the graphene-water interface through molecular dynamics simulations and showed that the interfacial thermal resistance could be reduced by 40% with the addition of a superlattice structure.

In this paper, the interfacial thermal resistance of graphene and different liquids at different temperatures is investigated. The graphene-water model, graphene-ethanol model, and graphene-ethylene glycol model are established to explore the interfacial thermal resistance under different conditions by adjusting the temperature and length of the liquid cluster during heat transfer. This work could provide new ideas for nano-microchannel thermal transport.

2. Calculation method

All simulations are performed using the Lammps program package,[42] employing Tersoff potential functions to describe C-C covalent interactions in graphene.[43-45] A simple point charge model (q-SPC/Fw)[46] modified by the original parameterization is used to describe the interactions within the water molecule, a model that is highly accurate for thermodynamic and kinetic calculations.[47] The polymer consistent force field (PCFF) described the internal interactions for ethanol and glycol clusters. The thermal transport properties of organic materials are investigated using the PCFF force field, and the results obtained were in good agreement with the experiments.[48-52] The Lorentz-Berthelot mixing principle calculated van der Waals forces using the Lennard-Jones (LJ) potential function.

$$\varepsilon_{ij} = \sqrt{\varepsilon_i \varepsilon_j}; \sigma_{ij} = \frac{\sigma_i + \sigma_j}{2} \quad (1)$$

where ε represents the Energy constant and σ represents the distance constant of the LJ potential function. The truncation distance is taken to be 9Å for all LJ potential functions.

In this paper, non-equilibrium molecular dynamics simulation (NEMD) is used.[53] Its simulation model is shown in Fig. 1, where a fixed layer is set at both ends, and the heat source heat sink is fixed at a temperature respectively to establish the temperature difference and form the heat flux. As shown in Fig. 2, there will be a temperature dip ΔT between the graphene and the liquid, and by counting the heat flow, the heat flow density J can be calculated, and the interface thermal resistance can be calculated as:

$$R = \frac{\Delta T}{J} \quad (2)$$

This paper investigates three models, as shown in Fig. 1, the graphene-water model, the graphene-ethanol model, and the graphene-ethylene glycol model. The initial size of the simulation box is 42 Å × 42 Å × 130 Å. Periodic boundary conditions are used in all directions,[54] and the time step is set to 0.5 fs. The structures are first optimized using energy minimization commands. An initial optimization is performed to correct any unreasonable structure parts and relieve internal stresses. The internal stresses are further relieved at an atmospheric pressure using NPT (constant mass, pressure, and temperature) system relaxation for 50 ps (100000-time steps). This is followed by a further 150 ps (300,000-time steps) relaxation at NVE (constant mass, volume, and Energy) using a Langevin heat bath to relieve the internal stresses fully. Finally, the heat transfer is carried out in the NVE (constant mass, volume, and energy) system using a Langevin heat bath with heat and cold source for 3000 ps (6,000,000 time steps), and the heat flow and temperature distribution are counted to calculate the interface thermal resistance.

3. Results and Discussion

Eleven temperature points between the freezing and boiling points of water are used and the thermal resistance of the interface between graphene and water at these temperatures is calculated based on the heat flow between the cold and heat sources. Fig. 3(a) shows that the interfacial thermal resistance is lower at temperatures close to the freezing and boiling points of the water and higher at intermediate temperature points. The calculated interfacial thermal resistance ranges

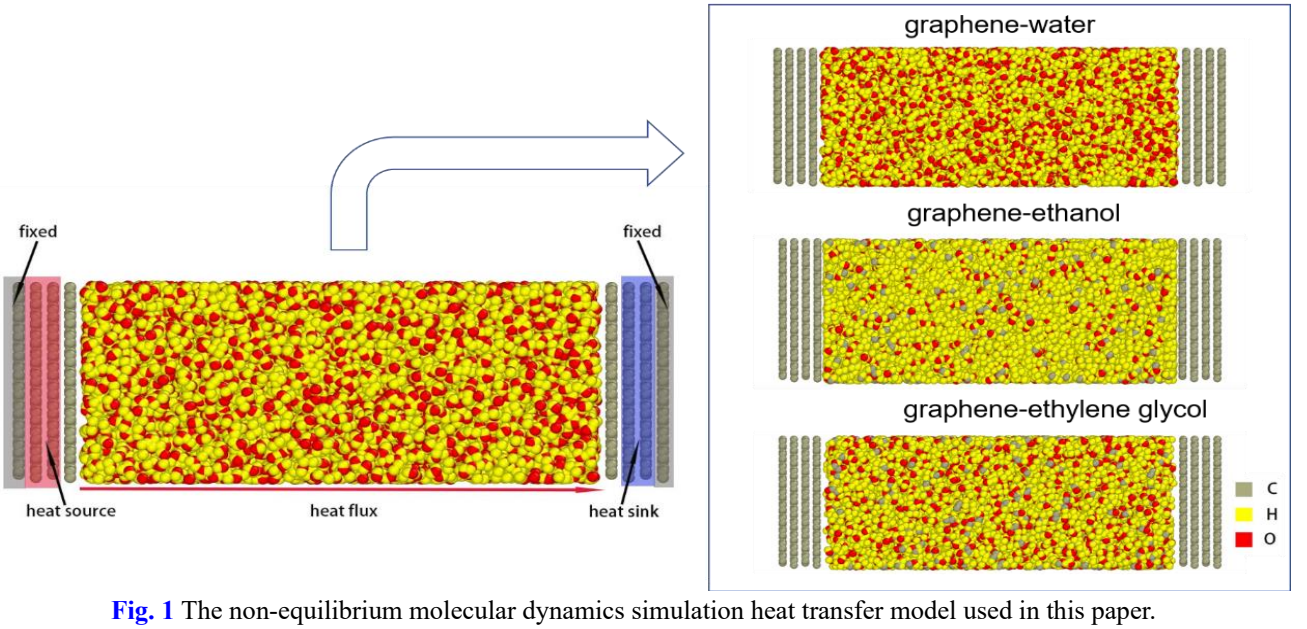

Fig. 1 The non-equilibrium molecular dynamics simulation heat transfer model used in this paper.

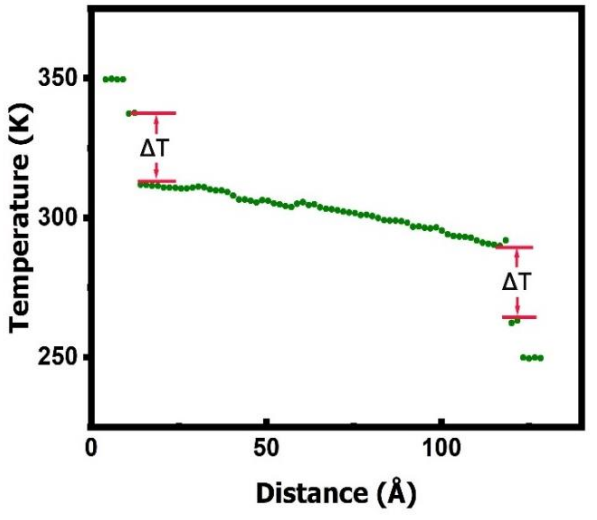

Fig. 2 Temperature plunge formed on the surface of the graphene in contact with the liquid.

from 2.05 × 10^{-8} m^2K/W to 2.61 × 10^{-8} m^2K/W, which is consistent with the reported thermal resistance of graphene-water: ~2.72 × 10^{-8} m^2K/W from Cao *et al.*,[55] ~3.21 × 10^{-8} m^2K/W from Ma *et al.*[34] and ~2.93 × 10^{-8} m^2K/W from Alexeev *et al.*[56]

In order to elucidate the mechanism of thermal resistance change, the phonon density of states (PDOS)[57,58] between graphene and liquid was obtained by Fourier transforming the velocity autocorrelation function.

$$D(\omega) = \int_0^{\tau_0} \frac{[v(0)\times v(t)]}{[v(0)\times v(0)]} exp(-2\pi i\omega t)dt \quad (3)$$

where $D(\omega)$ is the phonon density of states (PDOS) in conducting heat conduction, and $v(t)$ and $v(0)$ are the velocities of the particle at each moment and the initial moment, respectively.

As shown in Fig. 4(a), the difference in PDOS for the water clusters is not significant. This is because the range of change in the interfacial thermal resistance between water-graphene with temperature is not large and the intrinsic mechanistic changes cannot be well described using phonon density of state analysis. Near-wall density analysis[59] is used to elucidate the thermal resistance variation pattern. We investigated the water mass density and found that it comprises three distinct regions. These are the density fluctuation layer near the hot end of the graphene, the density fluctuation layer near the cold end of the graphene, and the intermediate density uniformly distributed layer, as shown in Fig. 5(a), respectively. The higher the density of water molecules in the near-wall region, the better the phonon

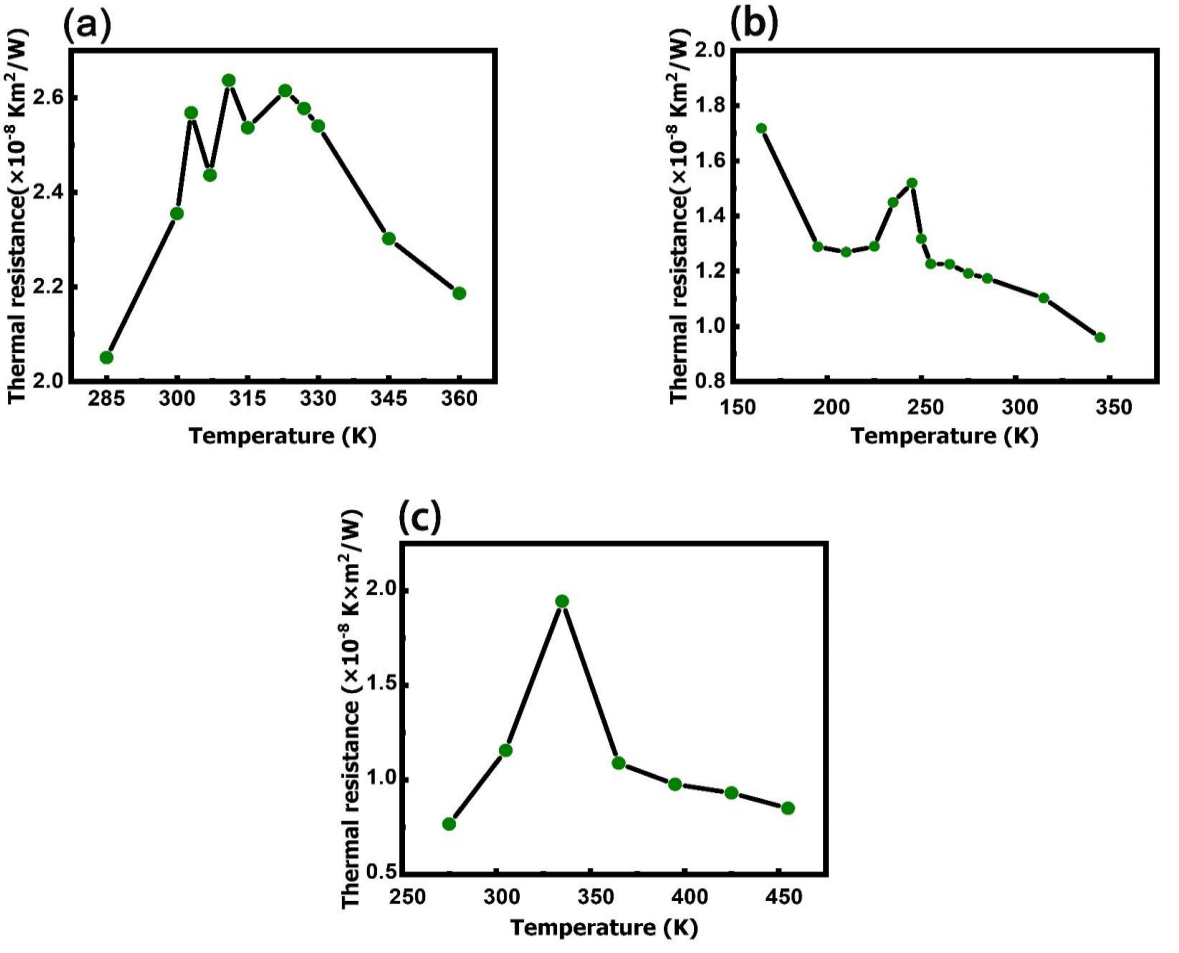

Fig. 3 Trend of thermal resistance of graphene- liquid interface with temperature (a) Graphene-water structure. (b) Graphene-ethanol structure. (c) Graphene-ethylene glycol structure.

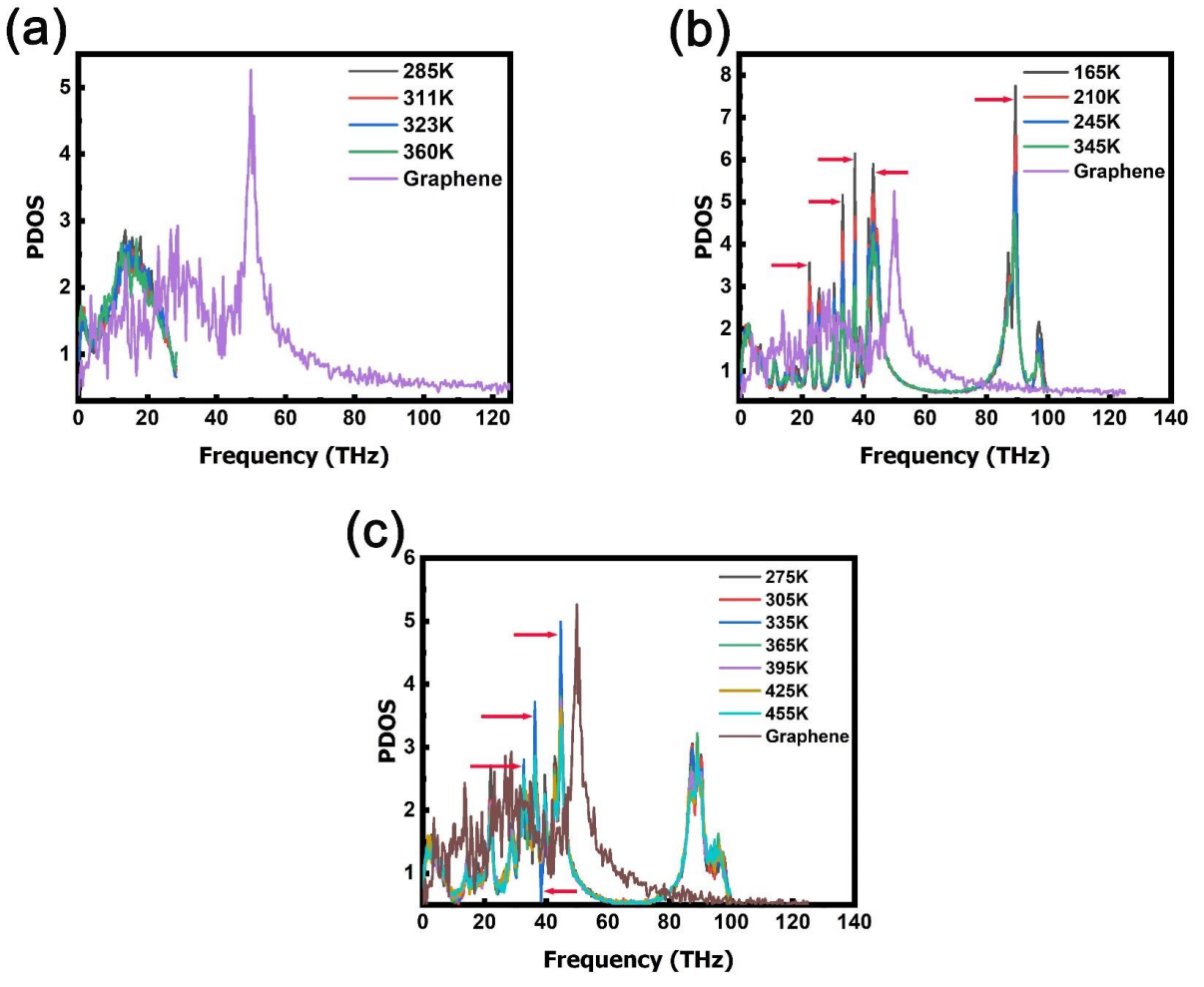

Fig. 4 PDOS diagram of graphene- liquid structure at different temperatures (a) Graphene-water structure. (b) Graphene-ethanol structure. (c) Graphene-ethylene glycol structure.

coupling can be produced and the lower the thermal resistance of the interface. From Fig. 5(b), it can be seen that the density of water clusters in the near-wall region is low in the temperature range of 303K to 330K, which makes the phonon coupling between water and graphene poorer, resulting in a higher thermal resistance at the interface.[60] At temperatures of 285 K and 360 K, the density of water clusters in the near-wall region is higher, making the interaction between water and graphene closer, resulting in a lower thermal resistance at the interface. To investigate the underlying mechanism of the changes of interfacial thermal resistances, we further calculate the interfacial binding energy of these systems. As shown in Fig. 6(a), the interfacial energy of the structure is lower at temperatures of 303 K to 330 K. This indicates that the binding energy of graphene and water clusters is low in this temperature range, resulting in a large interfacial thermal resistance.

To explain the pattern of change in more detail, we have taken thirteen temperature points between the melting and boiling temperatures of ethanol. To check the correctness of the results, we counted the temperature gradient of the ethanol cluster in the structure and the heat flow density of the cross-section, and the thermal conductivity of the ethanol cluster was calculated from Fourier's heat transfer law. This result agrees well with the experimental results.[61]

The calculated interfacial thermal resistance is shown in Fig. 3(b). It can be seen that the thermal resistance is higher near the freezing temperature of ethanol. With the increase in temperature, the thermal resistance shows a temporary decrease. Then, the temperature continues to increase. The thermal resistance becomes higher before it reaches a high point at 245 K. When the temperature continues to increase, the interfacial thermal resistance primarily decreases. To illustrate the reason for this phenomenon, we calculated the PDOS and interface energy of the system. Fig. 4(b) shows that the graphene PDOS and ethanol PDOS overlap more in the 20-50 THz range, indicating that graphene and ethanol are primarily coupled in the middle and high-frequency vibrations. Compared to water, ethanol is less vibrated in the low frequency, mainly around 40 THz, and is more coupled with graphene vibrations, which is also the reason for the lower thermal resistance of the ethanol and graphene interface. The arrow in Fig. 4(b) shows a higher peak in the PDOS of the ethanol cluster at 165 K. This indicates that there is more mismatch between the ethanol and graphene phonon vibrations at this temperature, making the interface thermal

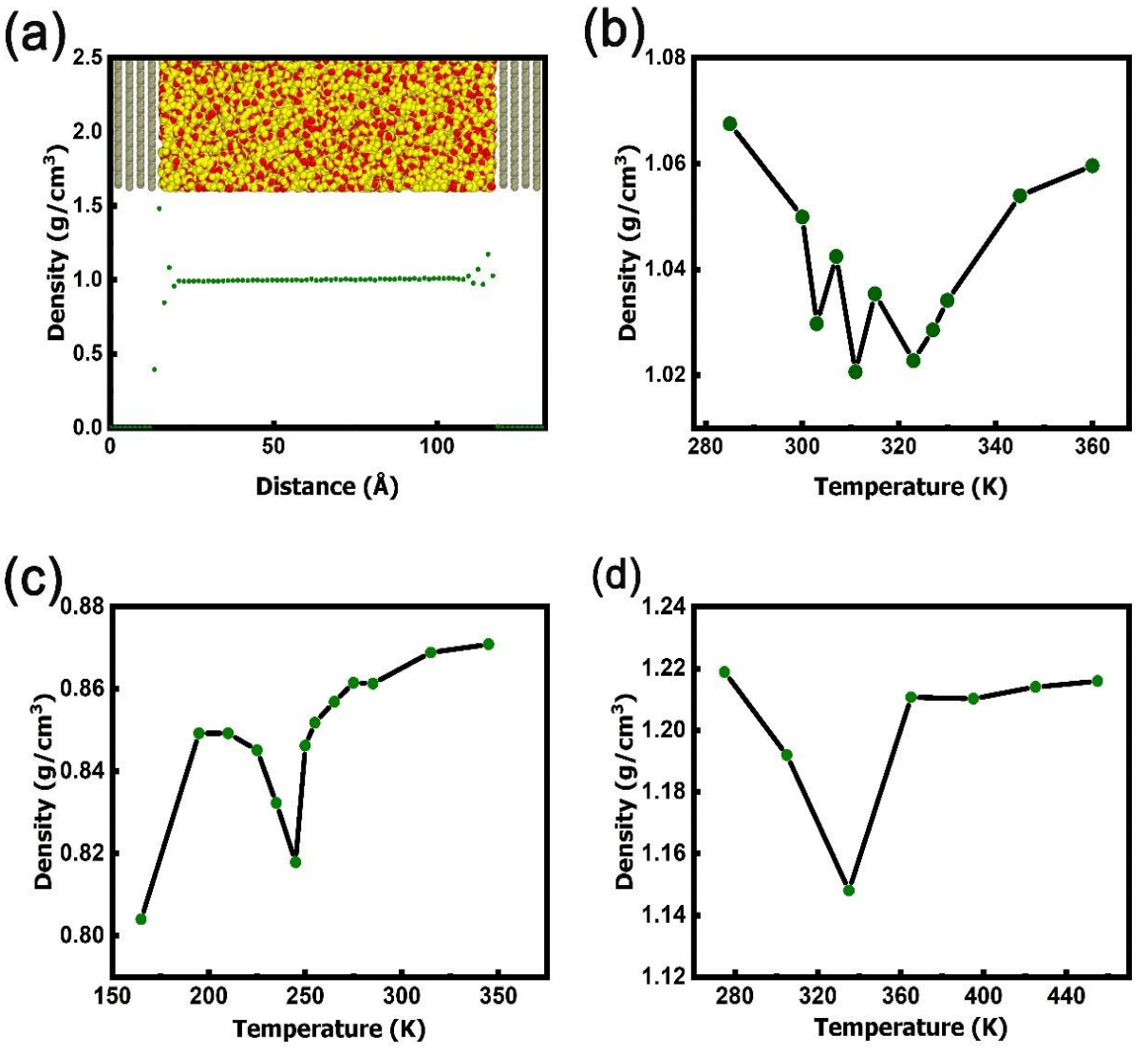

Fig. 5 Near-wall density analysis (a) Density distribution of liquid in the structure. (b) Density near the wall of graphene-water structure at different temperatures. (c) Density near the wall of graphene- ethanol structure at different temperatures. (d) Density near the wall of graphene- ethylene glycol structure at different temperatures.

resistance higher.[60] As shown in Fig. 5(c) and Fig. 6(b), the interfacial binding energy of graphene and ethanol is low and the ethanol cluster has a smaller density at the end near the graphene at a temperature of 165 K, which results in a lower energy transfer efficiency and a higher interfacial thermal resistance. At 345 K, the PDOS of ethanol and the PDOS of graphene overlap the most, indicating a higher degree of vibrational coupling between the ethanol cluster and graphene, As shown in Fig. 5(c) and Fig. 6(b), the higher interfacial binding energy between graphene and ethanol and higher near-wall density of ethanol clusters at a temperature of 345 K, indicating a stronger interaction between graphene and ethanol. In this case, resulting in a lower interfacial thermal resistance. Seven temperature points are taken between the freezing and boiling points of ethylene glycol. To verify the correctness of the simulation, we partitioned the glycol cluster in the structure into 50 boxes to calculate the temperature gradient inside the ethanol cluster and combined this with the previously calculated heat flow density to calculate the thermal conductivity of the ethanol cluster via Fourier's heat transfer law. We can find the thermal conductivity of ethylene glycol to be 0.243 W/m/K. This agrees well with the experimental results.[61] As shown in Fig. 3(c), the interfacial thermal resistance is lower near the freezing point of the glycol, and the interfacial thermal resistance of the glycol and graphene increases and then decreases with increasing temperature, which shows the opposite property of ethanol. The maximum interfacial thermal resistance is 1.94×10^{-8} m^2K/W at 335 K. The arrows in Fig. 4(c) show more prominent peaks in the PDOS of the glycol clusters at 335 K, indicating that the lower degree of vibrational coupling of glycol to graphene at this temperature results in a higher interfacial thermal resistance. As shown in Fig. 5(d) and Fig. 6(c), the lowest interfacial binding energy between graphene and glycol and low near-wall density of glycol clusters at a temperature of 335 K, which reflects the lowest interfacial

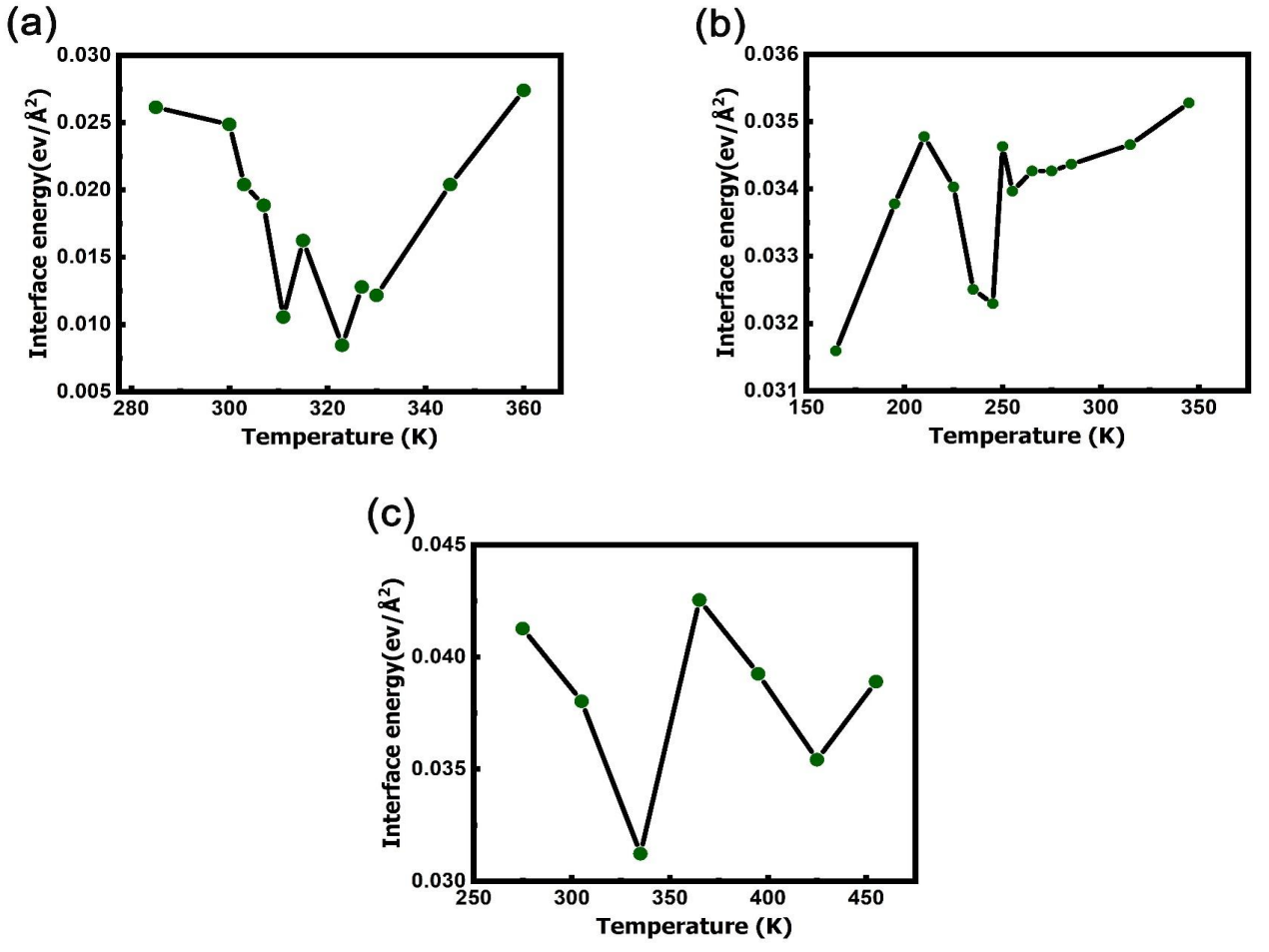

Fig. 6 Trend of interface energy of graphene-liquid structure with temperature (a) Graphene-water structure. (b) Graphene-ethanol structure. (c) Graphene-ethylene glycol structure.

energy transfer efficiency at this point and results in a higher interfacial thermal resistance. At other temperature points, the PDOS of the glycol cluster shows a better match with graphene, and the interface energy is also higher, indicating that better phonon coupling is produced and high energy transfer efficiency, which reduces the interfacial thermal resistance.

As shown in Fig. 6, the interfacial binding energy in the graphene-water structure is generally less than in the other two structures, which indicates that the energy transport efficiency between graphene-water is lower than in the other two structures, which results in the interfacial thermal resistance of the graphene-water structure being generally greater than the other two structures.

We further explored the effect of graphene width on the solid-liquid interfacial thermal resistance (ITR), and from Fig. 7, we can see that the interfacial thermal resistance of ethanol glycol and graphene does not vary much with graphene width, but the thermal resistance between water and graphene is decreasing as the graphene width increases. This is because graphene has a long phonon mean free-range, reported to be 775 nm for graphene,[62] expanding the graphene width. This increases the phonon mean free range of graphene, allowing for more excellent thermal conductivity between graphene and water. Since the degree of interfacial coupling between ethanol glycol and graphene is much better than that of water, expanding the graphene width has little effect on the thermal resistance.

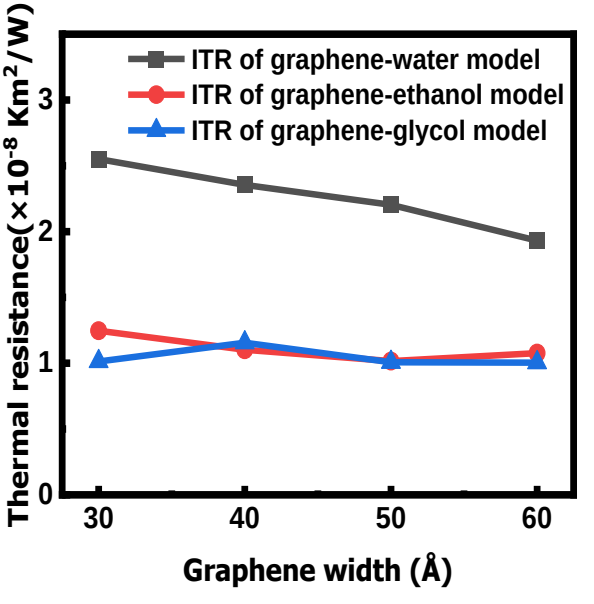

Fig. 7 Thermal resistance of the interface between three liquids and different widths of graphene.

Because the simulated model is still tiny compared to the experimental model, it is necessary to investigate the effect of liquid cluster thickness on the interfacial thermal resistance (ITR) and take different liquid thicknesses to study the interfacial thermal resistance between the liquid and graphene. As shown in Fig. 8, the interfacial thermal resistance between water and graphene does not change much with the increase in the thickness of the water cluster, while the two organic liquids have different degrees of increase in the interfacial thermal resistance with the increase in the thickness of the liquid cluster.

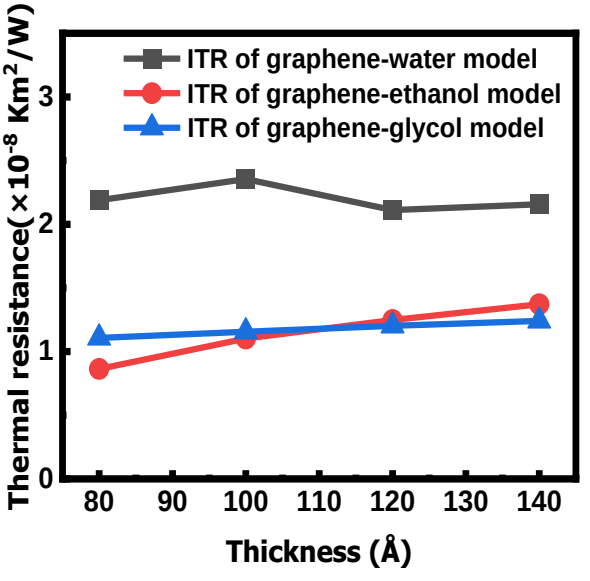

Fig. 8 Interfacial thermal resistance of three bodies with graphene at different thicknesses.

4. Conclusion

In summary, the thermal transport properties between graphene and water, ethanol, and ethylene glycol are investigated by a non-equilibrium molecular dynamics simulation (NEMD) approach. The results show that in the graphene-water model, the thermal resistance increases and decreases with increasing temperature decreases with increasing graphene width, and does not change significantly with increasing water cluster thickness. In the graphene-ethanol model, the thermal resistance is maximum around the freezing point and minimum around the boiling point, and the thermal resistance does not change much when the graphene width increases but increases simultaneously with the thickness of the ethanol cluster. In the graphene-glycol model, the thermal resistance increases and then decreases with increasing temperature, reaching a maximum at 335 K. The thermal resistance does not change much with increasing graphene width but increases slightly with expanding the thickness of the glycol cluster. As shown in this paper, we obtain the thermal transport properties of graphene and these three kinds of nanofluid at the interface, which is of great significance for efficient heat transfer of the solid-liquid interface.

Acknowledgement

This work was supported by the Basic Science Center Program for Ordered Energy Conversion of the National Natural Science Foundation of China (No. 51888103), National Natural Science Foundation of China (No. 51706039, 51606192 and 51720105007), Fundamental Research Funds for the Central Universities of China (Grant no. 2572020BF01) and the CAS Pioneer Hundred Talents Program.

Conflict of Interest

The authors declare no conflict of interest.

Supporting information

Not applicable.

References

[1] J. P. Mendez, F. Macias, M. P. Ariza, Thermal stability of tilt grain boundaries in graphene, *Applied Mechanics and Materials*, 2013, **481**, 129-132, doi: 10.4028/www.scientific.net/amm.481.129.

[2] J. Liu, H. Qin, Y. Liu, Multi-scale structure-mechanical property relations of graphene-based layer materials, *Materials*, 2021, **14**, 4757, doi: 10.3390/ma14164757.

[3] S. K. Samal, M. K. Moharana, Thermo-hydraulic and entropy generation analysis of recharging microchannel using water-based graphene-silver hybrid nanofluid, *Journal of Thermal Analysis and Calorimetry*, 2021, **143**, 4131-4148, doi: 10.1007/s10973-020-09382-8.

[4] H. Wang, S. Hu, K. Takahashi, X. Zhang, H. Takamatsu, J. Chen, Experimental study of thermal rectification in suspended monolayer graphene, *Nature Communications*, 2017, **8**, 15843, doi: 10.1038/ncomms15843.

[5] J.-H. Liu, H.-H. Xie, Y.-D. Hu, X. Zhang, Y.-Y. Zhang, Thermal transport in suspended SWCNTs at high heat fluxes, *International Journal of Heat and Mass Transfer*, 2017, **108**, 572-576, doi: 10.1016/j.ijheatmasstransfer.2016.12.059.

[6] S. Xu, A. Fan, H. Wang, X. Zhang, X. Wang, Raman-based nanoscale thermal transport characterization: a critical review, *International Journal of Heat and Mass Transfer*, 2020, **154**, 119751, doi: 10.1016/j.ijheatmasstransfer.2020.119751.

[7] J. S. Gan, H. Yu, M. K. Tan, A. K. Soh, H. A. Wu, Y. M. Hung, Performance enhancement of graphene-coated micro heat pipes for light-emitting diode cooling, *International Journal of Heat and Mass Transfer*, 2020, **154**, 119687, doi: 10.1016/j.ijheatmasstransfer.2020.119687.

[8] T. Ambreen, A. Saleem, M. Tanveer, K. Anirudh, S. A. Shehzad, C. W. Park, Irreversibility and hydrothermal analysis of the MWCNTs/GNPs-based nanofluids for electronics cooling applications of the pin-fin heat sinks: Multiphase Eulerian-Lagrangian modeling, *Case Studies in Thermal Engineering*, 2022, **31**, 101806, doi: 10.1016/j.csite.2022.101806.

[9] R. Avinash Kumar, M. Kavitha, P. Manoj Kumar, S. Arvindh Seshadri, Numerical study of graphene-platinum hybrid nanofluid in microchannel for electronics cooling, *Proceedings of the Institution of Mechanical Engineers, Part C: Journal of*

Mechanical Engineering Science, 2021, **235**, 5845-5857, doi: 10.1177/0954406220987261.
[10] M. Jamshidmofid, A. Abbassi, M. Bahiraei, Efficacy of a novel graphene quantum dots nanofluid in a microchannel heat exchanger, *Applied Thermal Engineering*, 2021, **189**, 116673, doi: 10.1016/j.applthermaleng.2021.116673.
[11] Y.-H. Chen, H.-S. Tao, D.-X. Yao, W.-M. Liu, Kondo metal and ferrimagnetic insulator on the triangular kagome lattice, *Physical Review Letters*, 2012, **108**, 246402, doi: 10.1103/physrevlett.108.246402.
[12] X.-L. Zhang, L.-F. Liu, W.-M. Liu, Quantum anomalous Hall effect and tunable topological states in 3d transition metals doped silicene, *Scientific Reports*, 2013, **3**, 2908, doi: 10.1038/srep02908.
[13] Z. Jiang, R. Li, S.-C. Zhang, W. Liu, Semiclassical time evolution of the holes from Luttinger Hamiltonian, *Physical Review B*, 2005, **72**, 045201, doi: 10.1103/physrevb.72.045201.
[14] W. Lai, Y.-Q. Ma, L. Zhuang, W. M. Liu, Photovoltaic effect of atomtronics induced by an artificial gauge field, *Physical Review Letters*, 2019, **122**, 223202, doi: 10.1103/physrevlett.122.223202.
[15] Y.-X. Zhen, M. Yang, R.-N. Wang, Thermoelectricity in B_{80}-based single-molecule junctions: first-principles investigation, *Frontiers of Physics*, 2019, **14**, 23603, doi: 10.1007/s11467-018-0865-0.
[16] R.-N. Wang, G.-Y. Dong, S.-F. Wang, G.-S. Fu, J.-L. Wang, Impact of contact couplings on thermoelectric properties of anti, Fano, and Breit-Wigner resonant junctions, *Journal of Applied Physics*, 2016, **120**, 184303, doi: 10.1063/1.4967751.
[17] Y.-J. Zhang, R.-N. Wang, G.-Y. Dong, S.-F. Wang, G.-S. Fu, J.-L. Wang, Mechanical properties of 1*T*-, 1*T*'-, and 1*H*-MX_2 monolayers and their 1*H*/1*T*'-MX_2 (M = Mo, W and X = S, Se, Te) heterostructures, *AIP Advances*, 2019, **9**, 125208, doi: 10.1063/1.5128849.
[18] S. Gbadamasi, M. Mohiuddin, V. Krishnamurthi, R. Verma, M. W. Khan, S. Pathak, K. Kalantar-Zadeh, N. Mahmood, Interface chemistry of two-dimensional heterostructures - fundamentals to applications, *Chemical Society Reviews*, 2021, **50**, 4684-4729, doi: 10.1039/d0cs01070g.
[19] O. V. Gendelman, J. Paul, Kapitza thermal resistance in linear and nonlinear chain models: Isotopic defect, *Physical Review E*, 2021, **103**, 052113, doi: 10.1103/physreve.103.052113.
[20] Y. Quan, S. Yue, B. Liao, Impact of electron-phonon interaction on thermal transport: a review, *Nanoscale and Microscale Thermophysical Engineering*, 2021, **25**, 73-90, doi: 10.1080/15567265.2021.1902441.
[21] I. N. Adamenko, K. E. Nemchenko, I. V. Tanatarov, Transmission and reflection of phonons and rotons at the superfluid helium-solid interface, *Physical Review B*, 2008, **77**, 174510, doi: 10.1103/physrevb.77.174510.
[22] G. Chen, Non-Fourier phonon heat conduction at the microscale and nanoscale, *Nature Reviews Physics*, 2021, **3**, 555-569, doi: 10.1038/s42254-021-00334-1.
[23] S. E. Kim, F. Mujid, A. Rai, F. Eriksson, J. Suh, P. Poddar, A. Ray, C. Park, E. Fransson, Y. Zhong, D. A. Muller, P. Erhart, D. G. Cahill, J. Park, Extremely anisotropic van der Waals thermal conductors, *Nature*, 2021, **597**, 660-665, doi: 10.1038/s41586-021-03867-8.
[24] Z. Wei, Y. Chen, C. Dames, Negative correlation between in-plane bonding strength and cross-plane thermal conductivity in a model layered material, *Applied Physics Letters*, 2013, **102**, 011901, doi: 10.1063/1.4773372.
[25] I. Jo, M. T. Pettes, J. Kim, K. Watanabe, T. Taniguchi, Z. Yao, L. Shi, Thermal conductivity and phonon transport in suspended few-layer hexagonal boron nitride, *Nano Letters*, 2013, **13**, 550-554, doi: 10.1021/nl304060g.
[26] E. Zanchini, A. Jahanbin, Effects of the temperature distribution on the thermal resistance of double u-tube borehole heat exchangers, *Geothermics*, 2018, **71**, 46-54, doi: 10.1016/j.geothermics.2017.07.009.
[27] Y.-K. Su, S.-C. Wei, L.-S. Chang, R.-L. Wang, C. J. Wang, Thermal resistance variation of HBT with high junction temperature and bias condition, *Solid-State Electronics*, 2003, **47**, 2113-2116, doi: 10.1016/s0038-1101(03)00216-8.
[28] J. Chen, X. Xu, J. Zhou, B. Li, Interfacial thermal resistance: past, present, and future, *Reviews of Modern Physics*, 2022, **94**, 025002, doi: 10.1103/revmodphys.94.025002.
[29] H. T. Aller, X. Yu, A. Wise, R. S. Howell, A. J. Gellman, A. J. H. McGaughey, J. A. Malen, Chemical reactions impede thermal transport across metal/β-Ga_2O_3 interfaces, *Nano Letters*, 2019, **19**, 8533-8538, doi: 10.1021/acs.nanolett.9b03017.
[30] C. Cancellieri, E. A. Scott, J. Braun, S. W. King, R. Oviedo, C. Jezewski, J. Richards, F. La Mattina, L. P. H. Jeurgens, P. E. Hopkins, Interface and layer periodicity effects on the thermal conductivity of copper-based nanomultilayers with tungsten, tantalum, and tantalum nitride diffusion barriers, *Journal of Applied Physics*, 2020, **128**, 195302, doi: 10.1063/5.0019907.
[31] J.-L. Barrat, F. Chiaruttini, Kapitza resistance at the liquid—solid interface, *Molecular Physics*, 2003, **101**, 1605-1610, doi: 10.1080/0026897031000068578.
[32] S. Srinivasan, S. R. Das, G. Balasubramanian, Transient evaporation of water thin film over nanostructured graphene, *Applied Surface Science*, 2019, **495**, 143545, doi: 10.1016/j.apsusc.2019.143545.
[33] H. Han, C. Schlawitschek, N. Katyal, P. Stephan, T. Gambaryan-Roisman, F. Leroy, F. Müller-Plathe, Solid-liquid interface thermal resistance affects the evaporation rate of droplets from a surface: a study of perfluorohexane on chromium using molecular dynamics and continuum theory, *Langmuir*, 2017, **33**, 5336-5343, doi: 10.1021/acs.langmuir.7b01410.
[34] Y. Ma, Z. Zhang, J. Chen, K. Sääskilahti, S. Volz, J. Chen, Ordered water layers by interfacial charge decoration leading to an ultra-low Kapitza resistance between graphene and water, *Carbon*, 2018, **135**, 263-269, doi: 10.1016/j.carbon.2018.04.030.
[35] J. Amrit, A. Ramiere, Kapitza resistance between superfluid helium and solid: role of the boundary, *Low Temperature Physics*, 2013, **39**, 752-755, doi: 10.1063/1.4821076.
[36] H. Song, F. Kang, Recent progress on thermal conduction of graphene, *Acta Physico Chimica Sinica*, 2021, **37**, 2101013-2101028, doi: 10.3866/pku.whxb202101013.

[37] D. Konatham, A. Striolo, Thermal boundary resistance at the graphene-oil interface, *Applied Physics Letters*, 2009, **95**, 163105, doi: 10.1063/1.3251794.
[38] J. Liu, F. Wang, L. Zhang, X. Fang, Z. Zhang, Thermodynamic properties and thermal stability of ionic liquid-based nanofluids containing graphene as advanced heat transfer fluids for medium-to-high-temperature applications, *Renewable Energy*, 2014, **63**, 519-523, doi: 10.1016/j.renene.2013.10.002.
[39] A. T. Pham, M. Barisik, B. Kim, Interfacial thermal resistance between the graphene-coated copper and liquid water, *International Journal of Heat and Mass Transfer*, 2016, **97**, 422-431, doi: 10.1016/j.ijheatmasstransfer.2016.02.040.
[40] H. Babaei, P. Keblinski, J. M. Khodadadi, Molecular Dynamics Study of the Interfacial Thermal Conductance at the Graphene/Paraffin Interface in Solid and Liquid PhasesVolume 4: Heat and Mass Transfer Under Extreme Conditions; Environmental Heat Transfer; Computational Heat Transfer; Visualization of Heat Transfer; Heat Transfer Education and Future Directions in Heat Transfer; Nuclear Energy. July 14-19, 2013. Minneapolis, Minnesota, USA. *American Society of Mechanical Engineers*, 2013, 55508, doi: 10.1115/ht2013-17478.
[41] X. Peng, P. Jiang, Y. Ouyang, S. Lu, W. Ren, J. Chen, Reducing Kapitza resistance between graphene/water interface via interfacial superlattice structure, *Nanotechnology*, 2022, **33**, 035707, doi: 10.1088/1361-6528/ac2f5c.
[42] S. Plimpton, Fast parallel algorithms for short-range molecular dynamics, *Journal of Computational Physics*, 1995, **117**, 1-19, doi: 10.1006/jcph.1995.1039.
[43] L. Lindsay, D. A. Broido, Optimized Tersoff and Brenner empirical potential parameters for lattice dynamics and phonon thermal transport in carbon nanotubes and graphene, *Physical Review B*, 2010, **81**, 205441, doi: 10.1103/physrevb.81.205441.
[44] J.-H. Zou, Z.-Q. Ye, B.-Y. Cao, Phonon thermal properties of graphene from molecular dynamics using different potentials, *The Journal of chemical physics*, 2016, **145**, 134705, doi: 10.1063/1.4963918.
[45] L. A. Girifalco, M. Hodak, R. S. Lee, Carbon nanotubes, buckyballs, ropes, and a universal graphitic potential, *Physical Review B*, 2000, **62**, 13104-13110, doi: 10.1103/physrevb.62.13104.
[46] F. Paesani, W. Zhang, D. A. Case, T. E. Cheatham 3rd, G. A. Voth, An accurate and simple quantum model for liquid water, *The Journal of chemical physics*, 2006, **125**, 184507, doi: 10.1063/1.2386157.
[47] T. I. Mizan, P. E. Savage, R. M. Ziff, Critical point and coexistence curve for a flexible, simple point-charge water model, *The Journal of Supercritical Fluids*, 1997, **10**, 119-125, doi: 10.1016/s0896-8446(97)00006-5.
[48] L. Hu, T. Desai, P. Keblinski, Determination of interfacial thermal resistance at the nanoscale, *Physical Review B*, 2011, **83**, 195423, doi: 10.1103/physrevb.83.195423.
[49] S. Shenogin, A. Bodapati, L. Xue, R. Ozisik, P. Keblinski, Effect of chemical functionalization on thermal transport of carbon nanotube composites, *Applied Physics Letters*, 2004, **85**, 2229-2231, doi: 10.1063/1.1794370.
[50] S. Shenogin, L. Xue, R. Ozisik, P. Keblinski, D. G. Cahill, Role of thermal boundary resistance on the heat flow in carbon-nanotube composites, *Journal of Applied Physics*, 2004, **95**, 8136-8144, doi: 10.1063/1.1736328.
[51] T. C. Clancy, T. S. Gates, Modeling of interfacial modification effects on thermal conductivity of carbon nanotube composites, *Polymer*, 2006, **47**, 5990-5996, doi: 10.1016/j.polymer.2006.05.062.
[52] J. Liu, M. Alhashme, R. Yang, Thermal transport across carbon nanotubes connected by molecular linkers, *Carbon*, 2012, **50**, 1063-1070, doi: 10.1016/j.carbon.2011.10.014.
[53] G. Ciccotti, M. Ferrario, Dynamical non-equilibrium molecular dynamics, *Entropy*, 2013, **16**, 233-257, doi: 10.3390/e16010233.
[54] P. C. Howell, Thermal conductivity calculation with the molecular dynamics direct method I: more robust simulations of solid materials, *Journal of Computational and Theoretical Nanoscience*, 2011, **8**, 2129-2143, doi: 10.1166/jctn.2011.1935.
[55] B.-Y. Cao, J.-H. Zou, G.-J. Hu, G.-X. Cao, Enhanced thermal transport across multilayer graphene and water by interlayer functionalization, *Applied Physics Letters*, 2018, **112**, 041603, doi: 10.1063/1.5018749.
[56] D. Alexeev, J. Chen, J. H. Walther, K. P. Giapis, P. Angelikopoulos, P. Koumoutsakos, Kapitza resistance between few-layer graphene and water: liquid layering effects, *Nano Letters*, 2015, **15**, 5744-5749, doi: 10.1021/acs.nanolett.5b03024.
[57] S. Lin, M. J. Buehler, The effect of non-covalent functionalization on the thermal conductance of graphene/organic interfaces, *Nanotechnology*, 2013, **24**, 165702, doi: 10.1088/0957-4484/24/16/165702.
[58] J. M. Dickey, A. Paskin, Computer simulation of the lattice dynamics of solids, *Physical Review*, 1969, **188**, 1407-1418, doi: 10.1103/physrev.188.1407.
[59] M. Barisik, A. Beskok, Temperature dependence of thermal resistance at the water/silicon interface, *International Journal of Thermal Sciences*, 2014, **77**, 47-54, doi: 10.1016/j.ijthermalsci.2013.10.012.
[60] J. Chen, G. Zhang, B. Li, Tunable thermal conductivity of $Si_{1-x}Ge_x$ nanowires, *Applied Physics Letters*, 2009, **95**, 073117, doi: 10.1063/1.3212737.
[61] N. B. Vargaftik, Handbook of Thermal Conductivity of Liquids and Gases, Boca Raton: CRC Press,1993.
[62] R. Su, X. Zhang, Size effect of thermal conductivity in monolayer graphene, *Applied Thermal Engineering*, 2018, **144**, 488-494, doi: 10.1016/j.applthermaleng.2018.08.062.

Author Information

Hao Chen *is a master student at College of Mechanical and Electrical Engineering, Northeast Forestry University, China. He is now a visiting student at Institute of Engineering Thermophysics, Chinese Academy of Sciences. His research focuses on micro-scale heat transfer.*

Ming Yang *is an associate professor at the Institute of Engineering Thermophysics, Chinese Academy of Sciences, China. His research focuses on micro-scale heat transfer, concentrated solar power applications and topological materials. He graduated from Institute of Physics, Chinese Academy of Sciences and obtained PhD degree in theoretical physics in 2015. In 2018-2019, he was a visiting scholar in University of Colorado at Boulder.*

Degao Qiao *is a master student at College of Mechanical and Electrical Engineering, Northeast Forestry University, China. He is now a visiting student at Institute of Engineering Thermophysics, Chinese Academy of Sciences. His research focuses on solar interface evaporation.*

Xingli Zhang *is an associate professor at Department of mechanical engineering drawing office, College of Mechanical and Electrical Engineering, China. She graduated from Harbin Institute of Technology in 2012. Her research interests include theoretical and computational approaches to model, simulate, and measure thermal and thermo-mechanical processes in nanostructures.*

Hang Zhang *is a professor in Institute of Engineering Thermophysics, Chinese Academy of Sciences and University of Chinese Academy of Sciences, in China. His research focuses on mechanisms and advanced technology on energy transport and conversions in emerging materials and equipment. He received his PhD degree in Physics from University of California, Riverside and then joined Caltech as a postdoctoral scholar.*